Journal of Theoretical and Applied Information Technology
30th April 2018. Vol.96. No 8

ISSN: 1992-8645 www.jatit.org E-ISSN: 1817-3195

PEDESTRIAN USING CATADIOPTRIC SENSOR

[12]BOUI MAROUANE, [2]HADJ-ABDELKADER HICHAM, [2]ABABSA FAKHR-EDDINE, [1]ABOUYAKHF EL HOUSSINE

[1] LIMIARF University Mohammed V-Rabat
[2] IBISC, University of Evry, France

E-mail: marouane.boui@ufrst.univ-evry.fr, hicham.hadjabdelkader@univ-evry.fr, fakhr-eddine.ababsa@ufrst.univ-evry.fr, bouyakhf@mtds.com

ABSTRACT

We investigate the detection of person in the omnidirectional images, adopting a linear SVM. We have implemented HOG-based descriptors, for omnidirectional and spherical images. In this paper we studied the influence of each parameter in our algorithm on the performances of person detections in catadioptric images. However, few studies have elaborated the problem of human detection using this type of cameras; therefore we have set up our own test base. Our results show that our detector can robustly detect people in omnidirectional images, as soon as the algorithm is adapted to the distortions introduced by the use of the omnidirectional camera.

Keywords: *Omnidirectional Sensor, HOG, Human Detection, Spherical Images Spherical Images Spherical Images.*

1. INTRODUCTION

This Human tracking is a highly processed research subject in computer vision, as it is the main part of several applications such as surveillance video systems, human-machine interaction and benchmarking applications. Omnidirectional cameras are useful for person detection and tracking, since they expand the field of view to 360o. Furthermore, they are well modelized [1] and already used in many applications like visual control [2], robot navigation, visual SLAM and motion estimation [3], [4]. The human detection in perspective images was wildly studied by the computer vision community. Several methods have been implemented; a survey summarizing the most popular ones is given in [5]. However, few works have been proposed omnidirectional image based per-son detection. Dupuis et al. [6], propose face detection in panoramic image obtained by unwrapping the omnidirectional image, to allow a better detection with viola and Jones algorithm. In [7]], the authors used HOG for person detection in panoramic image. However, the image processing for these approaches are directly applied in panoramic image and thus not adapted to the geometry of omnidirectional camera. Recently, Cinaroglu et al propose in [8] to adapt the image processing to the geometry of omnidirectional image using the Riemannian metric in order to improve the detection process. Nevertheless, the learning phase is based on perspective image database. Usually, human detection in images is based on gradient. In [18] the authors propose HOG descriptor and show that it significantly outperforms other methods for human detection. In order to increase the performances of the pedestrian detection, HOG algorithm was also combined with other descriptors like LBP [10].

Felzenszwalb et al [11] improved the robustness of HOG against partial occlusion using mixtures of deformable part models. Indeed there approach allows detection different parts of the human body through several windows. In order to use HOG for spherical images efficiently, an adequate metric for gradient computation is necessary. Several works have been done in this field. In, [12], the authors introduced the use of Riemannian metric to adapt the gradient computation in omnidirectional image. Shigang proposes in [13] a new spherical gradient operator based on centroidal spherical voronoi tessellation. This approach allows to define an adapted neighborhood for a point into the sphere, and hence to compute the gradient with high accuracy. In this paper, we propose to develop a new approach for human detection in omnidirectional image using the spherical representation. We first introduce a HOG-based descriptor, computed directly in the spherical space where an adapted gradient is used. To our

ISSN: 1992-8645 www.jatit.org E-ISSN: 1817-3195

knowledge, human detection approaches in omnidirectional image proposed in the literature, underestimate the nature of the database which is usually proposed for conventional camera. In the continuity of our work [9], we propose in this work an algorithm to generate an omnidirectional database from an existing perspective one. Indeed, the adapted database used for SVM training increases the performances of the person detection. This paper is organized as follows. In section 2, we first present the spherical model valid for the most omnidirectional cameras. Then we show how the omnidirectional database is generated from an existing perspective one. The last part of this section concerns the adaptation of HOG descriptor for spherical image geometry. In section 3, we present the real experimental results for our human detection approach. Section 4 gathers conclusions and suggestions for future research.

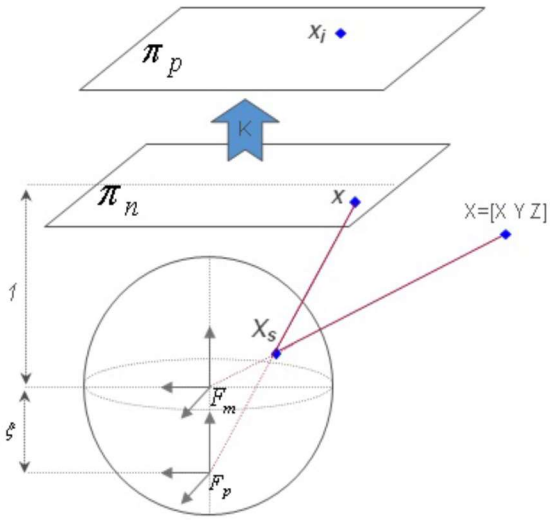

Figure 1: Unit Sphere Model

2. METHODOLGY

In this section, we first present briefly the generic model for all central cameras (conventional and non-conventional) based on the unit sphere. Then our approach is divided in two parts. The first part shows how we generate the omnidirectional database from an existing perspective database. The second one concerns the adaptation of the HOG descriptor for spherical image.

2.1 Unified spherical model

Sections Geyer et al proposed in [14] a generic model for omnidirectional image formation. This model is defined by a central projection onto unitary sphere, followed by a perspective projection onto an image plane. This model takes into account the mirror parameter (ξ) and the intrinsic camera parameters K. Fig.1. shows the unit sphere model where F_m and F_p are the projection centers of the mirror and the camera respectively.
The projection of a 3D point is then described by:
1- Projection of a 3D point X on the sphere according to the mirror reference coordinate frame:

$$(X)F_m \rightarrow (X_S)F_m = \frac{X}{\|X\|} = (X_S, Y_S, Z_S) \quad (1)$$

2- Changing the reference center $C_m \rightarrow C_p$

$$(X_S)F_m \rightarrow (X_S)F_p = (X_S, Y_S, Z_S + \xi) \quad (2)$$

3- Projected into the normalized plane

$$m = \left(\frac{X_S}{Z_S + \xi}, \frac{Y_S}{Z_S + \xi}, 1\right) = h(\chi_S) \quad (3)$$

4- Changing from image plan to pixelic image plan:

$$\boldsymbol{P} = km = \begin{bmatrix} f & f\eta\alpha & u_0 \\ 0 & f\eta & u_0 \\ 0 & 0 & 1 \end{bmatrix} m \quad (4)$$

We note f the focal length, (u_0, v_0) the main point and α is the skew. the (ξ) parameter related to the geometry of omnidirectional camera can be obtained by calibration. Since the function f is bijective [15], any omnidirectional image can be warped onto the unit sphere through the inverse projection f^{-1} [16]:

$$f^{-1} = \begin{bmatrix} \frac{\xi + \sqrt{1 + (1 - \xi^2)(x^2 + y^2)}}{x^2 + y^2 + 1} x \\ \frac{\xi + \sqrt{1 + (1 - \xi^2)(x^2 + y^2)}}{x^2 + y^2 + 1} y \\ \frac{\xi + \sqrt{1 + (1 - \xi^2)(x^2 + y^2)}}{x^2 + y^2 + 1} - \xi \end{bmatrix} \quad (5)$$

$$f^{-1} = \begin{bmatrix} x \\ y \\ 1 - \frac{x^2 + y^2 + 1}{\xi + \sqrt{1 + (1 - \xi^2)(x^2 + y^2)}} \end{bmatrix} \quad (5)$$

This unified projection model is valid for any single point-of-view camera, including perspective

Journal of Theoretical and Applied Information Technology
30th April 2018. Vol.96. No 8

ISSN: 1992-8645 www.jatit.org E-ISSN: 1817-3195

cameras. Indeed, just take $\xi = 0$ to find a perspective projection (pinhole model). ξ is also the parameter whose value depends on the shape of the mirror. Finally, even if the fisheye camera is not unique, this projection model is a good approximation of the actual projection and can be used to model some cameras of this type [19]. The model introduced by [20] makes it possible to add radial and tangential distortion in the image formation model compared to other models present in the literature. Its model makes the calibration parameters easily identifiable and offers a good compromise between an overly generic model and an over-parameterization.

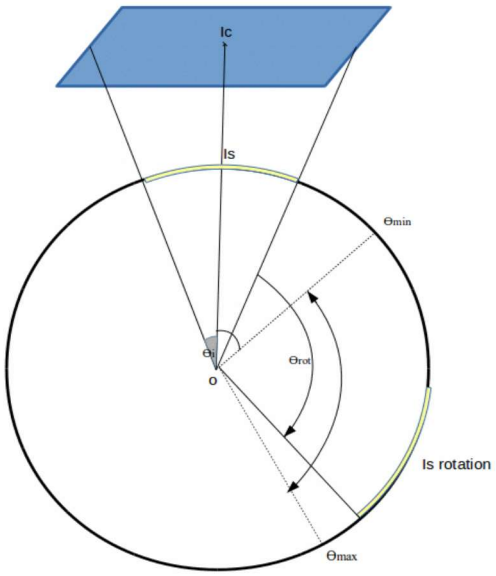

Figure 2: Diagram of the appropriate method

2.2 *Omnidirectional Database Generator (ODG)*

Image database has a central impact to enhance the efficiency of human detection algorithm. Several database for person detection are proposed in the literature. However, all of them are adapted for conventional images and no adapted database for omnidirectional image is proposed thus far. Within this scope, we propose a technique to create an adapted database for omnidirectional image, from any conventional database.

Let I_c be a perspective image of the conventional database. If we consider that image as a planar object observed by an omnidirectional camera, the corresponding omnidirectional image can be used for generating the adapted database. Indeed, the omnidirectional image of a person is generated by the omnidirectional camera. This hypothesis can be verified for a sufficient distance between the camera and the detected person.

(a) Perspective image

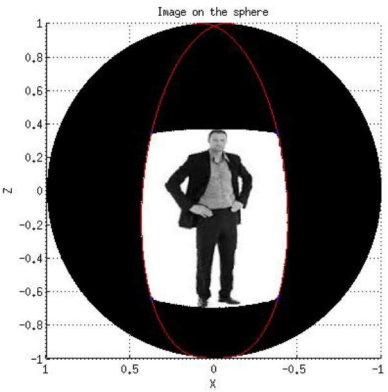

(b) Image on the sphere

Figure 3: Perspective image transformation to spherical image

The proposed technique is spelled out in the following steps:

First, a virtual perspective camera is defined for a given calibration parametersK_v. We will use K_v to move from the image I_c to the normalized plane I_n according to the standard pinhole model. Ic is defined at an adequate distance from the unit sphere and perpendicular to the axis passing through the north pole (as depicted in Fig.2). We assume a point Pn in the image I_n and a point P_c in the image I_c.

$$P_n = K_v^{-1} * P_c \quad (6)$$

We move from pixelized image I_c to normalized image $I_n(x_n, y_n, z_n)$. Then, the generated normalized image is projected onto the unit sphere to obtain a spherical image:

Then, the generated planar object is projected onto the spherical space using the unified projection model:

$$P_s = \frac{P_n}{||P_n||} \quad (7)$$

Journal of Theoretical and Applied Information Technology
30th April 2018. Vol.96. No 8

ISSN: 1992-8645 www.jatit.org E-ISSN: 1817-3195

We note that the adapted database is generated and defined on spherical space. Spherical space has the advantage of being invariant to rotation and therefore only one spherical image (θ, φ) is generated for each perspective image as can be seen in the figure (Figure 3). This will not be the case when we want to generate omnidirectional images. It will be necessary to distinguish between the rotations around the axis φ and the rotations around the axis θ. The rotation around the axis φ in the spherical space this translates into the omnidirectional image by a rotation around the center and which consequently does not modify the distortions created in the projected image. On the other hand, the rotations around the axis θ in the sphere will be reflected in the omnidirectional image by a movement from the center of the image to the outer circle (or the opposite) or in the omnidirectional image the distortions are not the same in the center of the omnidirectional image and on the edges.

To integrate this phenomenon into our omnidirectional image database, we define θmin, θmax which are the limits of the visibility zone of our omnidirectional image as in the figure (figure 2). Thus, we will use equations (6) and (7), to obtain our image $\boldsymbol{I}_o$ which represents the omnidirectional image as follows:

$$\boldsymbol{I}_o = K_{v0} * h\left(\begin{bmatrix}\cos(\theta) & -\sin(\theta) & 0\\ \sin(\theta) & \cos(\theta) & 0\\ 0 & 0 & 1\end{bmatrix} * \begin{bmatrix}\cos(\theta) & 0 & 0\\ 0 & \cos(\theta) & -\sin(\theta)\\ 0 & \sin(\theta) & \cos(\theta)\end{bmatrix}\right) \quad (8)$$

With K_{v0} the intrinsic parameters of our omnidirectional camera. The number of omnidirectional images generated from a single perspective image will be equal to θrot divided by the step we have chosen. As can be seen in the figure (Figure 4), the closer the image is to the edge, the larger the distortions.

2.3 Adapted HOG descriptor

Two HOG adaptation according to the gradient computation are proposed in this section. In the first one, the Riemannian metric is used. The second one consists on computing gradient directly in the spherical space.

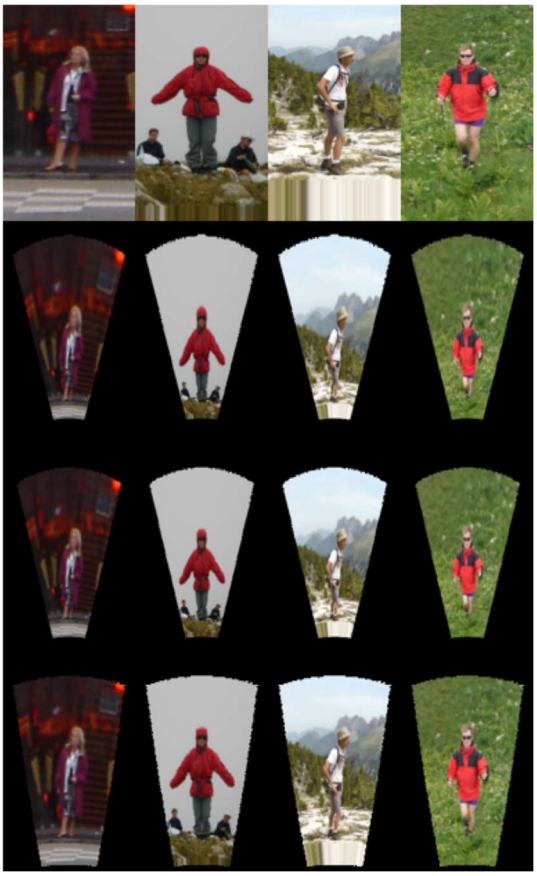

Figure 4: Perspective image transformation

2.3.1 Differential Operators on Riemannian Manifolds

In [17] and [12], the differential operator on the manifold is used to compute the gradient. Let $\mathcal{M}$ be a parametric surface on R_3 with an induced Riemannian metric g_{ij} that encodes the geometrical properties of the manifold. x^i is a local system of coordinates on $\mathcal{M}$. The gradient associated to a Riemannian metric is defined as follows:

$$\nabla f = \sum_{i=1}^{n}\sum_{j=1}^{n} g^{ij}\frac{\partial f}{\partial x^j}\frac{\partial}{\partial x^i} \quad (9)$$

Where g^{ij} is the inverse of the Riemannian metric g_{ij}. A point on the unit sphereS_2, it can be represented in Cartesian and polar coordinate by: $(X, Y, Z) = (sin\theta sin\phi, sin\theta cos\phi, cos\theta)$

ISSN: 1992-8645 www.jatit.org E-ISSN: 1817-3195

(a) Omnidirectional Image (b) Gradient compute with the Reimanienne Metric of the image (a) (c) Visualization of HOG

Figure 5: Example of HOG training in omnidirectional images.

The Euclidean line element is defined as follows:

$$dl^2 = dx^2 + dy^2 + dz^2 = d\theta^2(sin\theta)^2 d\phi \quad (10)$$

A point on the sphere is represented by (θ, ϕ) becomes after a polar stereographic projection a point (R, ϕ) in the image plane. The angle θ depends on the calibration parameters of our camera, while ϕ remain the same.
In the general case we have:

$$\theta = arctan\left(\frac{R\left(1+\xi+\sqrt{(1+\xi)^2 - R^2(\xi^2} \right.}{1+\xi-R^2\xi+\sqrt{(1+\xi)^2-R^2(}\right. \quad (11)$$

Thus the metric becomes:

$$dl = \frac{\left(\xi+\xi^2+\sqrt{(1+\xi)^2-R^2(\xi^2-1)}\right)^2}{\left(R^2 d\phi^2 + \frac{(1+\xi)dR^2}{1-R^2(\xi-1)+\xi}\right)}$$

$$dl^2 = \frac{}{(R^2+(1+\xi)^2)^2}$$

Using the identities: $R = x^2 + y^2$ and $\phi = tan^{-1}\left(\frac{y}{x}\right)$ we have:

$$dl^2 = \lambda\left(4(ydx - xdy)^2 - \frac{4(1+\xi)(xdx+ydy)^2}{(x^2+y^2)(\xi-1)-\xi-1}\right) \quad (13)$$

with:

$$\lambda = \frac{\left(\xi+\xi^2+\sqrt{(1+\xi^2)^2-(x^2+y^2)(\xi^2-}\right.}{4(x^2+y^2)(x^2+y^2+(1+\xi)^2)^2} \quad (14)$$

From (11) we can calculate g^{ij} and its inverse matrix g_{ij} we obtaine:

$$g^{ij} = \gamma\begin{pmatrix} -x^2(\xi-1)+\xi+1 & xy(\xi-1) \\ xy(\xi-1) & -y^2(\xi-1)+\xi+1 \end{pmatrix} \quad (15)$$

with:

$$\gamma = \frac{(x^2+y^2+(1+\xi)^2)^2}{(1+\xi)\left(\xi+\xi^2+\sqrt{1-(x^2+y^2)(\xi^2-1}\right.} \quad (16)$$

The Riemannian metric its speed computation, as can be seen as the weighting function of the conventional gradient computed in the omnidirectional image.Fig.5b shows the calculation of the omnidirectional gradient of a real omnidirectional image. Its HOG descriptor is shown in Fig.5c.

$$\nabla f = g^{ij}\frac{\partial f}{\partial x^j} \quad (17)$$

2.3.2 Calculation of spherical gradient in the spherical space.

The spherical gradient can be obtained knowing the perceived metric of a unit sphere $r = 1$ if $g^{ij} = \begin{pmatrix} 1 & 0 \\ 0 & sin\theta \end{pmatrix}$ then $g_{ij} = \begin{pmatrix} 1 & 0 \\ 0 & \frac{1}{sin\theta} \end{pmatrix}$
The spherical gradient is thus defined by:

$$\nabla_{s^2} I_s(\theta,\phi) = \frac{\partial I_s(\theta,\phi)}{\partial\theta}e_\theta + \frac{1}{sin\theta}\frac{\partial I_s(\theta,\phi)}{\partial\phi}e_\phi \quad (18)$$

Where (θ, ϕ) a spherical image is (θ, ϕ) are the

Journal of Theoretical and Applied Information Technology
30th April 2018. Vol.96. No 8

ISSN: 1992-8645 www.jatit.org E-ISSN: 1817-3195

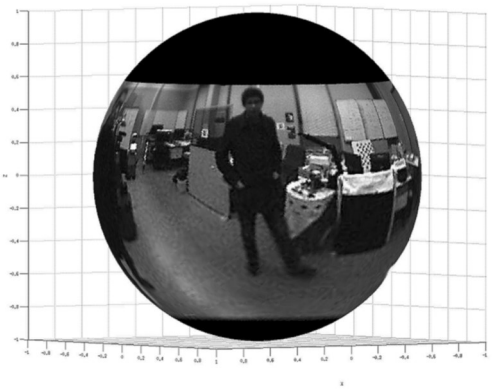

(a) Omnidirectional image projected onto the unit sphere

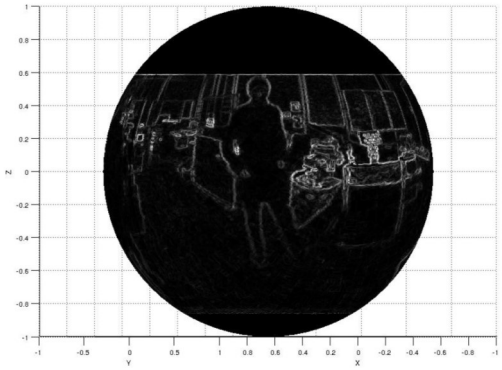

(b) spherical gradient of the image (a

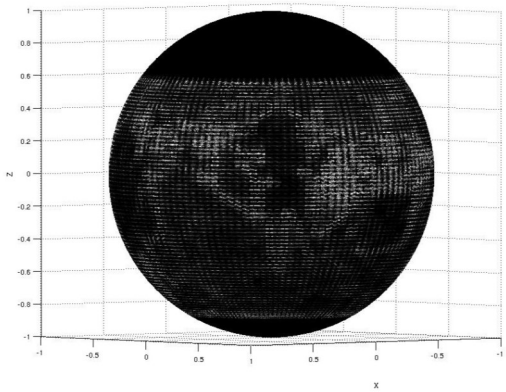

(c) Visualization of the spherical HOG calculated in the image (θ, φ)

Figure 6: Visualization of the spherical HOG calculated in the image(θ, φ)

longitude and colatitude angles respectively. e_θ and e_ϕ are the unit vector.

In practice, the gradient is computed using the first-

Order Image derivatives:

$$\left(\nabla_{S^2} I_s(\theta_j, \phi_k)\right)^2 = |I_s(\theta_{j+1}, \varphi_k) - I_s(\theta_j, \varphi_{k+1})|^2 + \frac{1}{sin^2(\theta_j)} |I_s(\theta_{j+1}, \varphi_{k+1}) - I_s(\theta_j, \varphi_{k+1})|^2 \quad (19)$$

Once the gradient is calculated on the sphere, we will be able to generate the HOG descriptor on the spherical space. Fig.6b shows the calculation of the spherical gradient of a real omnidirectional image. Its HOG descriptor is shown in Fig.6c. Example of HOG training in omnidirectional images.

3. EXERIMENTAL RESULTS

In order to validate our approach, we use the INRIA perspective database. During our experiments, we compare three methods Fig.8. The first method is based on using a classical HOG. For this method we use the INRIA database to train our linear SVM. In the second method, HOG is used with an adapted computation of the gradient to the omnidirectional image, through the Riemannian metric as in the work of [8] .

Using the proposed method ODG in the previous section, the learning phase for this method is based on the adapted training database generated by transforming positive perspective images of the INRIA database into omnidirectional images. Each perspective image generates 11 omnidirectional images, for the training stage; we have generate 16500 positive learning images. The calibration parameter of our virtual omnidirectional camera as well as the sampling size of the unit sphere was made such that a person on a certain distance with respect to the sensors has a reasonable view in the template. Negative images are generated using omnidirectional images.

For the learning phase of the third method based on the spherical gradient, the processing will be performed on the spherical images $I(\theta, \varphi)$. The advantage of this method is that during the transformation of perspectives positive images of INRIA database, a perspective image will generate a single spherical image. This is due to the fact that the spherical image is invariant to the rotation. So we will have 1500 positive images, the processing will thereafter be made on the spherical image.

ISSN: 1992-8645 www.jatit.org E-ISSN: 1817-3195

(a) Detection in unwrapped image

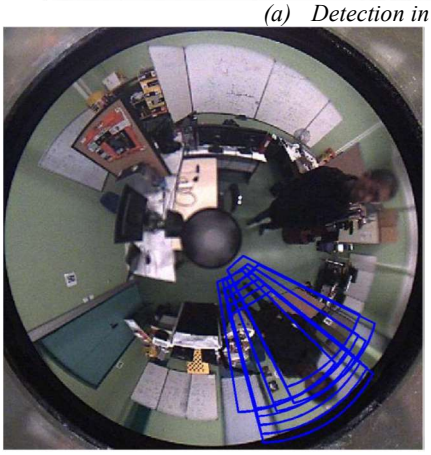

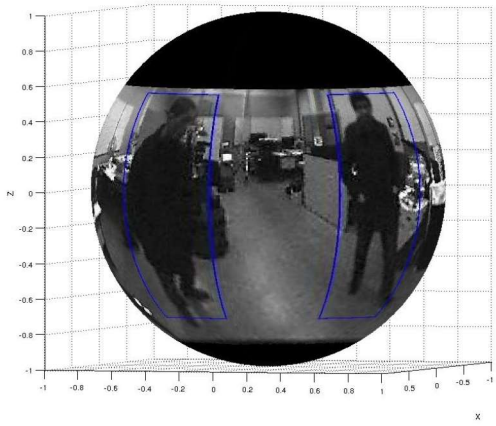

(a) Detection in omnidirectional image *(c) Detection with spherical HOG)*

Figure 8: Example of detection with the three methods

During the learning phase of SVM, we have divided the training database into two parts.

The first one allows us to make an initial learning, the second one helps us to reinforce that learning by performing a hard examples. These methods consist of testing SVM trained with the second part of the database image. Only poorly detected images will be reintegrated again in the learning database. For the test database we use 130 images acquired directly using an omnidirectional camera with hyperbolic mirror Fig.7 to quantify the performances of our detector, we relied on the curve Receiver Operating Characteristic (ROC) as shown in Fig.9.

To quantify the performance of our detector, we relied on the curve Receiver Operating Characteristic (ROC) as we can see in Figures 8-10, the x-axis represent the True positive rate $\left(recall\ or\ \frac{True\ Pos}{True\ Pos+False\ Neg}\right)$ and the y-axis the false positive rate value $\left(\frac{False\ Pos}{False\ Pos+True\ Neg}\right)$. It allows to easily comparing our three methods, taking into account the area under the curve (AUC).

For our database test all images have been marked with a suitable annotation.

A detected window is considered to be a true positive if it encroaches on an annotated box for at least 50% of its surface.

$$\frac{area(Detected\ Window \cap Annotated\ Box)}{area(Detected\ Window \cup Annotated\ Box)} > 0.5$$

It must be noted that the proposed detection methods, on the unit sphere, allow a significant improvement in performance of detections: 7.53% compared to the method based on the calculation of the gradient with the Riemann metric and 16.91% compared to the naive HOG method. We have also tested the different possibilities for the spherical detector, as we can see in Fig.11, on the three spherical descriptors, the one based on the sobel filter gives the best performances; it improves by 2% the detection in our database. We establish that the choice of the window size can be important in the setting up our descriptor. We found that the best

ISSN: 1992-8645 www.jatit.org E-ISSN: 1817-3195

performances are due to the use of 96x160 as can be seen in the Fig.10.

Figure 7: A catadioptric camera with an hyperbolic mirror.

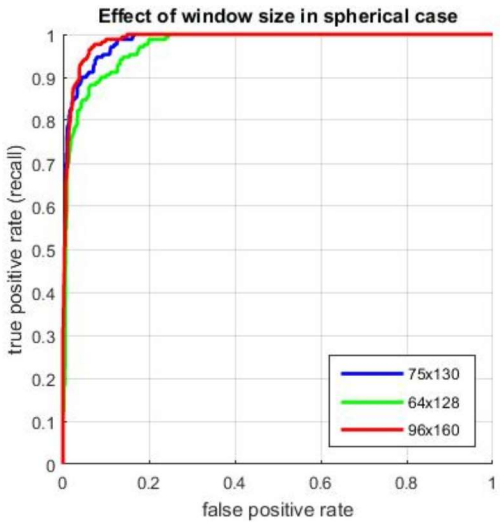

Figure 10: Effect of window size in spherical case.

Overall, we note that the proposed improvements which are adapting the database for the omnidirectional camera with our omnidirectional image generator and calculating HOG on the spherical image, allow efficient detection of persons on the spherical images, even if it is less efficient than the detections made by prospects methods on perspective images.

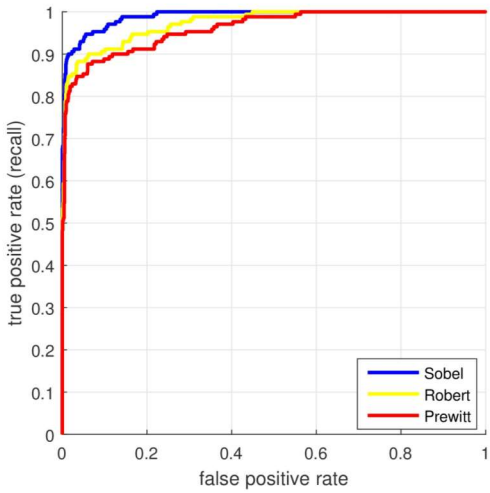

Figure 11: Effect of filter.

4. CONCLUSION

In this work we have described an efficient system for the 3D detection of people with an omnidirectional camera. using the spherical gradient combined with a conventional SVM. We presented our approach that allows a significant improvement in the performance of the HOG algorithm for the detection of people in omnidirectional images using the spherical representation. This is possible thanks to the use of the unified model. We have studied the influence of various descriptor parameters and concluded that filter and window size are important for good performance. The experimental results presented in this paper confirm the effectiveness and robustness of the proposed approach. Moreover during the implementation of the experimental part it was necessary to create an omnidirectional database for the tests we introduced a method for converting perspective images into omnidirectional image to transform a database perspective into a database omnidirectional data. So in the approach proposed during the learning step we do not need to create multiple images for a single perspective person depending on his position in the image, since the spherical image is invariant to the rotation. Future work has focused on the implementation of a larger database and the improvement of sampling during the transition from the omnidirectional space to the spherical space.

ISSN: 1992-8645 www.jatit.org E-ISSN: 1817-3195

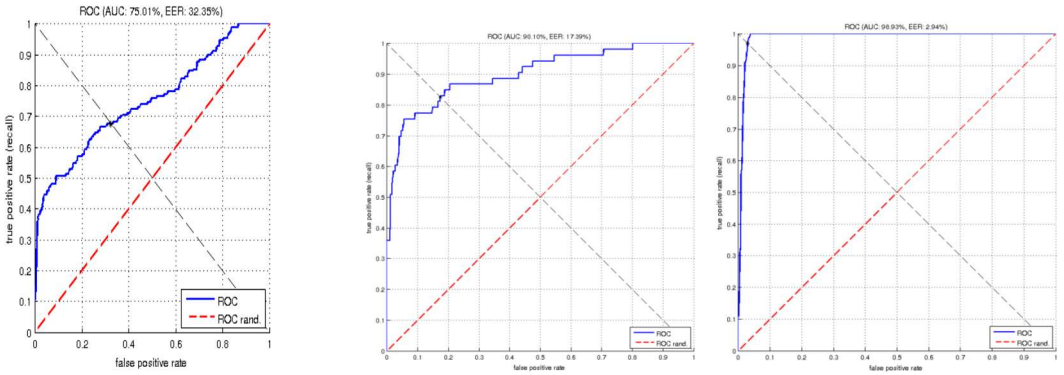

(a) Result Method 1 *(b) Result Method 2* *(c) Result Method 3*

Figure 9: Example of detection with the three methods

REFRENCES:

[1] Geyer, C., Daniilidis, K. (2000). A unifying theory for central panoramic systems and practical implications. In Computer Vision—ECCV 2000 (pp. 445-461). Springer Berlin Heidelberg.

[2] Hicham Hadj Abdelkader, Youcef Mezouar, Nicolas Andreff, and Philippe Martinet, "Image-based control of mobile robot with central catadioptric cameras," in Robotics and Automation, 2005. ICRA 2005. Proceedings of the 2005 IEEE International Conferenceon. IEEE, 2005, pp. 3522–3527.

[3] Alejandro Rituerto, Luis Puig, and Jose Jesus Guerrero, "Visual slam with an omnidirectional camera," in Pattern Recognition (ICPR), 2010 20th International Con-ference on. IEEE, 2010, pp. 348–351.

[4] Bazin, J. C., Demonceaux, C., Vasseur, P., Kweon, I. S. (2010). Motion estimation by decoupling rotation and translation in catadioptric vision.Computer Vision and Image Understanding, 114(2), 254-273.

[5] Dollar, P., Wojek, C., Schiele, B., Perona, P.(2012). Pedestrian detection: An evaluation of the state of the art. Pattern Analysis and Machine Intelligence, IEEE Transactions on, 34(4), 743-761.

[6] Dupuis, Y., Savatier, X., Ertaud, J. Y., Vasseur, P. (2013). Robust radial face detection for omnidirectional vision. Image Processing, IEEE Transactions on,22(5), 1808-1821.

[7] Hariyono, J., Hoang, V. D., Jo, K. H. (2015). Human Detection from Omnidirectional Camera Using Feature Tracking and Motion Segmentation. In Intelligent Information and Database Systems (pp. 329-338). Springer International Publishing.

[8] Cinaroglu, I., Bastanlar, Y. (2015). A direct approach for object detection with catadioptric omnidirectional cameras. Signal, Image and Video Processing, 1-8.

[9] Boui, M., Hadj-Abdelkader, H., Ababsa, F. E., Bouyakhf, E. H. (2016, September). New approach for human detection in spherical images. In Image Processing (ICIP), 2016 IEEE International Conference on (pp. 604-608). IEEE.

[10] Wang, X., Han, T. X., Yan, S. (2009, September). An HOG-LBP human detector with partial occlusion handling. In Computer Vision, 2009 IEEE 12th International Conference on (pp. 32-39). IEEE.

[11] Felzenszwalb, P. F., Girshick, R. B., McAllester, D. (2010, June). Cascade object detection with deformable part models. In Computer vision and pattern recognition (CVPR), 2010 IEEE conference on (pp. 2241-2248). IEEE.

[12] Bogdanova, I., Bresson, X., Thiran, J. P., Vandergheynst, P. (2007). Scale space analysis and active contours for omnidirectional images. Image Processing, IEEE Transactions on, 16(7), 1888-1901.

[13] Li, S. (2013). Spherical gradient operator. IEEJ Transactions on Electrical and Electronic Engineering, 8(S1), S61-S65.

[14] Geyer, C., Daniilidis, K. (2003, October). Mirrors in motion: Epipolar geometry and motion estimation. In Computer Vision, 2003. Proceedings. Ninth IEEE International Conference on (pp. 766-773). IEEE.

[15] BARRETO, Joao P. et ARAUJO, Helder. Geometric properties of central catadioptric line images and their application in calibration.

ISSN: 1992-8645 www.jatit.org E-ISSN: 1817-3195

Pattern Analysis and Machine Intelligence, IEEE Transactions on, 2005, vol. 27, no 8, p. 1327-1333.

[16] Hicham Hadj-Abdelkader, Ezio Malis, and Patrick Rives, "Spherical image processing for accurate visual odometry with omnidirectional cameras," in The 8th Workshop on Omnidirectional Vision, Camera Networks and Non-classical Cameras-OMNIVIS, 2008.

[17] Puig L., Guerrero, J. J., Daniilidis, K. (2014). Scale space for camera invariant features. Pattern Analysis and Machine Intelligence, IEEE Transactions on, 36(9), 1832-1846.

[18] Dalal, N., Triggs, B. (2005, June). Histograms of oriented gradients for human detection. In Computer Vision and Pattern Recognition, 2005. CVPR 2005. IEEE Computer Society Conference on (Vol. 1, pp. 886-893). IEEE.

[19] Ying, X., & Hu, Z. (2004, May). Can we consider central catadioptric cameras and fisheye cameras within a unified imaging model. In European Conference on Computer Vision (pp. 442-455). Springer, Berlin, Heidelberg.

[20] Mei, C., & Rives, P. (2007, April). Single view point omnidirectional camera calibration from planar grids. In Robotics and Automation, 2007 IEEE International Conference on (pp. 3945-3950). IEEE.